PORTLAND PRESS

Research Article

A frog cathelicidin peptide effectively promotes cutaneous wound healing in mice

Jing Wu[1],*, Jun Yang[1],*, Xiaofang Wang[1],*, Lin Wei[2], Kai Mi[1], Yan Shen[1], Tong Liu[1], Hailong Yang[1] and Lixian Mu[1]

[1]School of Basic Medical Sciences, Kunming Medical University, Kunming, Yunnan, China; [2]Jiangsu Key Laboratory of Infection and Immunity, Institutes of Biology and Medical Sciences, Soochow University, Suzhou, Jiangsu, China

Correspondence: Hailong Yang (jxauyhl@163.com) or Lixian Mu (mulixian77@163.com)

OPEN ACCESS

Although cathelicidins in mammals have been well characterized, little is known about the function of cathelicidin in amphibians. In the present study, a novel 24-residue peptide (cathelicidin-NV, ARGKKECKDDRCRLLMKRGSFSYV) belonging to the cathelicidin family was identified from the skin of the plateau frog *Nanorana ventripunctata*. Cathelicidin-NV showed strong wound healing-promoting activity in a murine model with a full-thickness dermal wound. It directly enhanced the proliferation of keratinocyte cells, resulting in accelerated re-epithelialization of the wound site. Cathelicidin-NV also promoted the proliferation of fibroblasts, the differentiation of fibroblasts to myofibroblasts and collagen production in fibroblasts, which are implicated in wound contraction and repair processes. Furthermore, cathelicidin-NV promoted the release of monocyte chemoattractant protein-1, tumor necrosis factor-α, vascular endothelial growth factor and transforming growth factor-β1 *in vivo* and *in vitro*, which are essential in the wound-healing processes such as migration, proliferation and differentiation. The MAPK (ERK, JNK and p38) signaling pathways were involved in the wound healing-promoting effect. Additionally, unlike other cathelicidins, cathelicidin-NV did not have any direct effect on microbes and showed no cytotoxicity and hemolytic activity toward mammalian cells at concentrations up to 200 μg/ml. This current study may facilitate the understanding of the cellular and molecular events that underlie quick wound healing in *N. ventripunctata*. In addition, the combination of these properties makes cathelicidin-NV an excellent candidate for skin wound therapeutics.

Introduction

The skin serves as a protective barrier against the outside world and any break in it must be rapidly and efficiently mended. Cutaneous wound healing is a highly orchestrated biological process, which is essential to restore the integrity of the skin barrier and is critical to the survival of the organism after injury. Among vertebrates, skins of amphibians are exposed to more dangers of biological or non-biological injuries than others [1]. Amphibians have evolved the capacity to respond to environmental challenges. Their skins, limbs or tails possess the excellent ability to heal and regenerate as needed for normal physiology and pathophysiology [2–4].

Cathelicidins are a family of antimicrobial and immune-stimulatory peptides found exclusively in vertebrates thus far. Two cathelicidins (Bac5 and Bac7) were first isolated from bovine neutrophils in 1989 [5], and then many cathelicidins have been identified from different species of mammals [6], birds [7], reptiles [8], amphibians [9] and fishes [10]. Mammalian cathelicidins are one of the best characterized classes of host defense peptides [11] and they have multifaceted roles in immune modulation, inflammation, wound healing [12], angiogenesis [13], cell death [14] and autoimmune disorders [15]. However, relatively limited research has been done about cathelicidins in amphibians (Anura, Caudata and Gymnophiona). As of April 2018, ~7858 amphibian species have been described

*These authors made equal contributions to this work.

in the AmphibiaWeb database (http://www.amphibiaweb.org/). The first amphibian cathelicidin (cathelicidin-AL) possessing antimicrobial activity was characterized in 2012 [16], and then eight additional cathelicidins (cathelicidin-RC1 and -RC2, Lf-CATH1 and -2, BG-CATH, cathelicidin-Bg, cathelicidin-PY and cathelicidin-PP) with antimicrobial and/or anti-inflammatory activities have been identified [9]. Currently, only two cathelicidins with wound-healing ability have been characterized in amphibians. One is tylotoin, which was isolated from the salamander *Tylototriton verrucosus* (Caudata: Salamandridae) [17]; the other is cathelicidin-OA1, which was identified from the Chinese odorous frog *Odorrana andersonii* (Anura: Ranidae) [18]. Additionally, two non-cathelicidin peptides (CW49 and AH90) from frog skin secretions and one designed peptide (tiger17) based on frog antimicrobial peptides, also showed wound-healing ability [19–21].

The plateau frog *Nanorana ventripunctata* is endemic to northwestern Yunnan province in China. It lives at high altitudes (3120–4100 m) with extremely cold weather. Thus, to survive, *N. ventripunctata* must respond rapidly and effectively to various biotic and abiotic damage, including cutaneous damage caused by ultraviolet radiation and cold. It would be useful to explore whether there are some molecules involved in wound healing in the skins of *N. ventripunctata*.

In the current study, a novel cathelicidin peptide named cathelicidin-NV was identified from the skin of the plateau frog *N. ventripunctata*. It showed potential wound healing-promoting activity in a murine model with a full-thickness dermal wound. The cytokines, chemokines and mitogen-activated protein kinases (MAPKs) (ERK, JNK and p38) signaling pathways that are involved in the wound healing-promoting effect were also studied. Our results suggest that cathelicidin-NV might be an excellent candidate for the development of a novel wound-healing agent.

Materials and methods

N. ventripunctata sample

Adult *N. ventripunctata* ($n = 30$; weight range 20–25 g) was collected from Shangri-La, Yunnan province of China. Skin secretions were collected as previously reported [9]. Frogs were stimulated with volatilized anhydrous ether immersed in absorbent cotton, and their skin surface was seen to exude secretions. Skin secretions were washed with 0.1 M phosphate buffer, pH 6.0 (PBS) [containing 1% (v/v) protease inhibitor cocktail, Sigma, P8340-5]. The collected solutions containing skin secretions were quickly centrifuged (10 000 *g* for 10 min) and the supernatants were lyophilized. The study was approved by the Animal Care and Use Ethics Committee of Kunming Medical University.

Peptide purification

The peptide purification procedures were performed according to the method described in our previous work [22]. An aliquot (1 *g*) of lyophilized skin secretion was dissolved in 10 ml of PBS and centrifuged at 5000 *g* for 10 min. The supernatant was applied to a Sephadex G-50 (Superfine, Amersham Biosciences) gel filtration column (2.6 cm diameter, 100 cm length) equilibrated with 0.1 M PBS for preliminary separation. Elution was performed with the same buffer, collecting fractions of 3.0 ml. The absorbance of the elute fractions were monitored at 280 nm. The cell proliferation activity was determined as described below. The fraction containing cell proliferation activity was further purified by a C_{18} reversed-phase high-performance liquid chromatography (RP-HPLC, Gemini C_{18} column, 5 μm particle size, 110 Å pore size, 250 mm length, 4.6 mm diameter) column. The elution is performed using a linear gradient of 0–80% acetonitrile containing 0.1% (v/v) trifluoroacetic acid in 0.1% (v/v) trifluoroacetic acid/water over 60 min, as illustrated in Figure 1B. UV-absorbing peaks were collected, lyophilized and assayed for cell proliferation activity. Peaks with cell proliferation activity were collected and lyophilized for a second HPLC purification procedure using the same conditions as illustrated in Figure 1C.

Primary structural analysis

The N-terminal sequence of the purified peptide was determined by Edman degradation on an Applied Biosystems pulsed liquid-phase sequencer (model ABI 491). Matrix-assisted laser desorption/ionization time-of-flight mass spectrometry (MALDI-TOF MS) was used to identify the purified peptide. The AXIMA CFR mass spectrometer (Kratos Analytical) was analyzed in the linear and the positive ion mode using an acceleration voltage of 20 kV and an accumulating time of single scanning of 50 s.
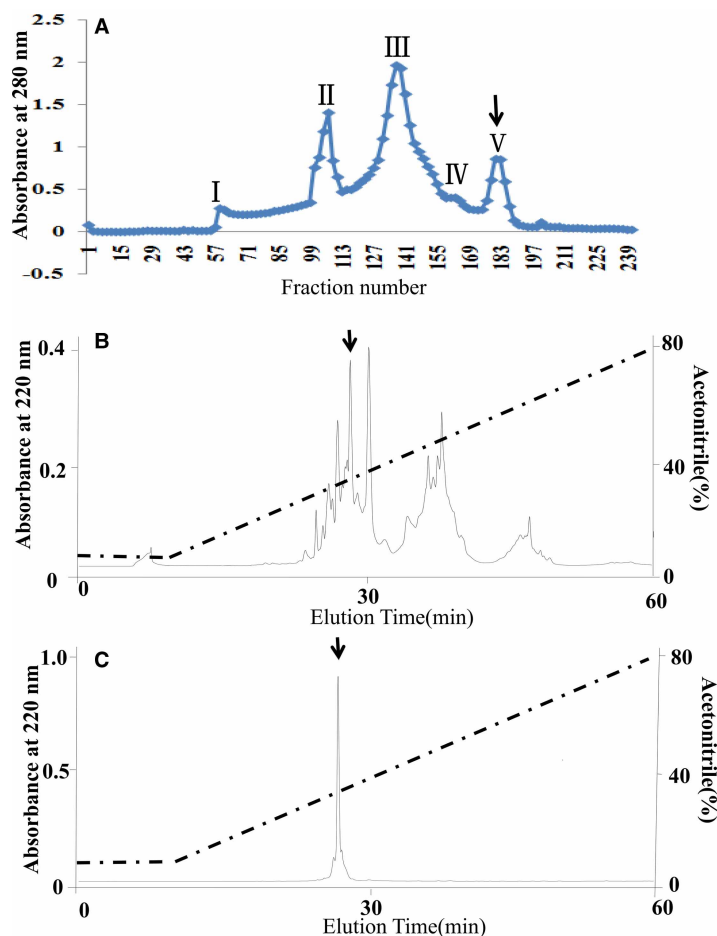
Figure 1. Purification of cathelicidin-NV from the skin secretions of *N. ventripunctata*.

(**A**) Sephadex G-50 gel filtration of skin secretions of *N. ventripunctata*. The skin secretions were applied to a Sephadex G-50 gel filtration column. The elution was performed by 0.1 M PBS, collecting fraction of 3.0 ml. The fraction containing cell proliferation activity is marked by an arrow. (**B**) The interesting fraction from the Sephadex G-50 gel filtration was further purified by a C_{18} RP-HPLC column. The elution was performed at a flow rate of 0.7 ml/min with the indicated gradient of acetonitrile in 0.1% (v/v) trifluoroacetic acid (TFA) in water. (**C**) The eluted peak (*arrow* in **B**) containing cell proliferation activity was further purified by a C_{18} RP-HPLC column. The purified cathelicidin-NV is indicated by an *arrow*.

cDNA cloning

The experiment was performed according to the method described in our previous work [22]. Total RNA was extracted from the skin of *N. ventripunctata* using the RNeasy Protect Mini Kit (QIAGEN, Germany) according to the manufacturer's instructions. An In-Fusion SMARTerTM Directional cDNA Library Construction Kit was used for cDNA synthesis. The synthesized cDNA was used as the template for PCR to screen the cDNAs encoding the peptide (cathelicidin-NV). According to the sequence determined by Edman degradation, an anti-sense degenerate primer (cathelicidin-NV-R1) was designed and coupled with a 5′ PCR primer (the adaptor sequence of the 3′ In-Fusion SMARTer CDS Primer provided in the kit) to screen the 5′ fragment of cDNA encoding cathelicidin-NV. Then, a sense primer (cathelicidin-NV-F1) was designed according to the 5′ coding region and coupled with the 3′ PCR primer from the library kit to screen the full-length cDNAs. The PCR conditions were 2 min at 95°C, and 30 cycles of 10 s at 92°C, 30 s at 50°C and 40 s at 72°C, followed by a 10 min extension at 72°C. The PCR products were cloned into pGEM®-T Easy vector (Promega, Madison, WI). DNA sequencing was performed on an Applied Biosystems DNA sequencer, model ABI PRISM 377. Primers used in this research are listed in the Supplementary Table S1.

Antimicrobial assay

Antimicrobial activity of cathelicidin-NV was assayed according to our previous methods [9]. Microorganisms were obtained from the First Affiliated Hospital of Kunming Medical University. The growth of the microbe was determined by monitoring the absorbance at 600 nm. The minimal concentrations at which no microbial growth occurred were recorded as MIC values.

Cytotoxicity and hemolysis

Cytotoxicity and hemolytic assay were performed according to the method described in our previous work [9]. Cytotoxicity against human skin fibroblasts (HSFs), human HaCat keratinocyte cells and murine macrophage cell line RAW264.7 was determined by the MTT assay. Cathelicidin-NV dissolved in serum-free RPMI 1640 medium was added to cells in 96-well plates (2×10^4 cells/well), and the serum-free RPMI 1640 medium without cathelicidin-NV was used as control. After incubation for 24 h, 20 μl of MTT solution (5 mg/ml) was added to each well, and the cells were further incubated for 4 h. Finally, cells were dissolved in 200 μl of Me_2SO_4, and the absorbance at 570 nm was measured. Rabbit erythrocyte suspensions were incubated with cathelicidin-NV and then the absorbance of the supernatant was measured at 540 nm. 1% (v/v) Triton X-100 and PBS were used as the positive and the negative control, respectively.

Cell proliferation assay

The proliferation of HSFs and immortalized human HaCat keratinocyte cells was measured using a colorimetric assay according to the method described in our previous work [17]. Cells were cultured in Dulbecco's modified Eagle's medium (DMEM; Invitrogen) supplemented with 10% fetal bovine serum (FBS) and penicillin (100 u/ml)–streptomycin (100 mg/ml) at 37°C in a humidified 5% CO_2 atmosphere, respectively. HaCat and HSF cells were plated into 96-well plates (2×10^4 cells/well), respectively. After adhering to the plate, cells were incubated with vehicle (DMEM) or cathelicidin-NV with different concentrations for 24 h. Based on previous reports, the amphibian cathelicidin (tylotoin) [17] and three non-cathelicidin peptides (CW49, AH90 and tiger17) from amphibians [19–21], as well as the sole human cathelicidin LL-37 [23], exhibited wound-healing ability with concentrations ranging from 100 ng/ml to 250 μg/ml. We optimized the concentration (2, 5, 10 and 20 μg/ml) of cathelicidin-NV to measure its activities. Then 20 μl of 3-(4,5-dimethylthiazol-2-yl)-2,5-diphenyl-2H-tetrazolium bromide (MTT) solution (R&D Systems Inc., Minneapolis, MN) was added to each well for a further 4 h incubation at 37°C. After the cells were washed three times with PBS (pH 7.4), the insoluble formazan product was dissolved by incubation with 150 μl of DMSO. The absorbance of each well was measured on an enzyme-linked immunosorbent assay (ELISA) micro-plate reader at 570 nm. The optical density reflects the level of cell metabolic activity. Each experiment was performed in triplicate.

In vitro wound assay

For wound assays in the presence of cathelicidin-NV, HaCat Cells were seeded into 6-well plates (1×10^6 cells/well) to confluence in DMEM supplemented with 10% FBS. After 12 h of serum starvation (DMEM supplemented with 1% FBS) for increasing the peptide sensitivity, the cell monolayer was then subjected to a mechanical scratch wound using a sterile pipette tip. After washing twice with PBS to remove detached cells, cells were then cultured for additional periods (from 0 to 48 h) in a serum-free basal medium in the continued presence of vehicle or cathelicidin-NV (20 μg/ml) and mitomycin C (5 mg/ml) to prevent cell proliferation.

The same fields of the wound margin were photographed using a Primovert microscope (Zeiss, Germany) at different time points (at 0, 24 and 48 h after scratch wounding). Cell migration activity was expressed as the percentage of the gap relative to the total area of the cell-free region immediately after the scratch, named the repair rate of scarification, using the Image J software (National Institutes of Health, Bethesda, MD, U.S.A.). For each plate, six randomly selected images were acquired. All experiments were carried out in triplicate.

Cytokine and chemokine measurements *in vitro*

Raw 264.7 murine macrophage cells were seeded and adhered to 96-well culture plates (2×10^4 cells/well). The cells were treated with cathelicidin-NV (2, 5, 10 and 20 μg/ml) or vehicle for 48 h; then culture supernatants were collected and assessed for MCP-1 (monocyte chemoattractant protein-1), TNF-α (tumor necrosis factor-α), VEGF (vascular endothelial growth factor) and TGF-β1 (transforming growth factor-β1) by using

ELISA kits (DAKAWE, Beijing, China). ELISA was performed according to the manufacturer's instructions. Experiments were independently carried out in triplicate.

Western blot analysis

Raw 264.7 murine macrophage cells were cultured in 6-well culture plates (2×10^6 cells/well) and transferred to serum-free DMEM for a 16-h incubation. The cells were incubated with cathelicidin-NV (2, 5, 10 and 20 μg/ml) or vehicle for 3 h. Then, the cells were washed twice with ice-cold phosphate-buffered saline (PBS) and lysed with RIPA lysis buffer (Beyotime, China). The proteins were extracted for western blot analysis according to our previously described method [15]. The concentration of protein was determined by the Bradford protein assay. Then the cellular proteins were separated on a 12% SDS–PAGE gel and electroblotted onto a polyvinylidene difluoride membrane. Primary antibodies against β-actin (1:5000, Santa Cruz Biotechnology, U.S.A.) and Erk1/2, SAPK/JNK and p38 MAPK (1:2000; Cell Signaling Technology, Beverly, MA, U.S.A.) were used in western blot analysis.

In vivo wound-healing experiments

It would be valuable to test the role of cathelicidin-NV in a frog model. However, the captured frogs in the wild are different in age, sex, size and body weight, which may lead to inaccurate results in the frog model of wound healing. Furthermore, commercial antibodies in frogs are not available for our further studies, including immunohistochemistry, ELISA and western blot analysis. A mouse model of wound healing was used to determine the activity of cathelicidin-NV. Kunming mice (6–7-week-old male) were anesthetized using 1% pentobarbital sodium (0.1 ml/20 g body weight). After the dorsal hairs were shaved by an electric clipper and the dorsal skin was cleansed with Betadine, two full-thickness skin wounds of 6-mm diameter were created independently on the back of each mouse using a biopsy punch, as previously reported [24]. After wounding, mice were caged individually until termination of the experiment. Mice were treated with vehicle, cathelicidin-NV (20 μl, 200 μg/ml) or EGF (20 μl, 100 μg/ml) applied directly to the wound site twice daily. To observe the natural course of wound healing in mice, the wounds were photographed on days 0 to 10 after the skin injury. Time-dependent alterations of the wound area are shown in Figure 4A. The wound areas were calculated from the photographs using PhotoShop (Adobe Photoshop Element 2.0, Adobe Systems) ($n = 10$ per group). The researchers performing the experiment and analysis were both blinded. The study was approved by the Animal Care and Use Ethics Committee of Kunming Medical University.

Cytokine and chemokine measurements *in vivo*

The biopsy specimens involving the central part of the wounds (days 0, 1, 2, 4 and 6) were obtained from mice for tissue ELISA. Skin specimens were homogenized in 4 ml 0.1 M PBS [containing 1% (v/v) protease inhibitor cocktail, Sigma, P8340-5]; then the homogenates were transferred to Eppendorf tubes and centrifuged at 13 000 g for 30 min at 4°C. The total protein concentrations were adjusted using the Bio-Rad protein assay dye (Bio-Rad Laboratories, Hercules, CA), and MCP-1, TNF-α, VEGF and TGF-β1 protein levels were determined using ELISA kits (DAKAWE, Beijing, China).

Histology and immunohistochemistry

At days 4 and 10 after wounding, mice were killed (five animals in each group, one paired wounds per animal), and the biopsy specimens involving the central part of the wounds were obtained from mice for light microscopy. Skin specimens were fixed in 4% paraformaldehyde for 24 h and then were dehydrated by washing with a series of ethanol solutions. Subsequently, skin specimens were cleared in xylene, and embedded in paraffin wax. Thick sections (5 μm) were prepared and stained with Hematoxylin and Eosin (H&E) for histological analysis. Thick sections (3 μm) were stained with the Masson collagen staining method to observe the collagen fibers. The IPLab imaging software (BD Biosciences, Bedford, MA) was used to measure the changes of the wound. Width of the wound and distance of the neo-epithelium were measured on H&E-stained sections, and percent re-epithelialization was calculated according to the following formula: (distance covered by neo-epithelium)/(distance between wound bed) $\times 100$ ($n = 5$ per group).

Immunohistochemistry was performed following standard procedures. A total of 3 μm sections were reacted with anti-α SMA primary antibody (1:1000 dilution, ab32575, abcam) after blocking endogenous peroxidase and nonspecific binding. Then, they were incubated with biotinylated goat anti-rabbit IgG (1:200 dilution,

ab150077, abcam) for 1 h at room temperature. As a control, sections were treated with the same dilution buffer without the primary antibodies.

Peptide synthesis

Cathelicidin-NV (ARGKKECKDDRCRLLMKRGSFSYV) and the scrambled version of cathelicidin-NV called sNV (KLSRGVCDKRDCASMRYFLKGREK), which are stabilized by one intramolecular disulfide bond between Cys7-Cys12, were synthesized by the peptide synthesizer GL Biochem Ltd (Shanghai, China). The synthetic peptides were purified and then analyzed by HPLC and MALDI-TOF MS to confirm that the purity was higher than 98%.

Statistical analysis

Statistical differences were determined using the one-way analysis of variance test or Student's t-test. $P < 0.05$ and $P < 0.01$ were considered statistically significant. Results are shown as mean ± SEM.

Results

Purification of cathelicidin-NV

As shown in Figure 1A, the skin secretions of *N. ventripunctata* were divided into five fractions after Sephadex G-50 gel filtration. Then the fraction containing activity to promote cell proliferation was pooled and subjected to a C_{18} RP-HPLC column for further purification (Figure 1B,C). The purified peptide with cell proliferation activity was named cathelicidin-NV (Figure 1C) (marked by an arrow). Unless indicated otherwise, the purified cathelicidin-NV was used in the experiments which are involved in the wound healing-promoting activities.

Characterization of cathelicidin-NV

After Edman degradation, the complete amino acid sequence of purified cathelicidin-NV was identified with the following sequence: ARGKKECKDDRCRLLMKRGSFSYV. Cathelicidin-NV is composed of 24 amino acid residues including two cysteines, which are possible to form an intramolecular disulfide bridge. MALDI-TOF MS analysis (Supplementary Figure S1) indicated that the molecular mass of cathelicidin-NV was 2845.9 Da. It is 1.47 Da lower than the calculated mass (2847.37 Da), suggesting that one disulfide bridge was formed by two cysteines in the mature peptide. The complete nucleotide sequence encoding the cathelicidin-NV precursor (GenBank accession number MH010580) and the encoded amino acid sequence are shown in Figure 2; the cathelicidin-NV precursor is composed of 146 amino acid residues, including a predicted 20 amino acid signal peptide and a conserved 102 amino acid cathelin domain, followed by a 24 amino acid mature peptide.

BLAST search indicated that the precursor is a member of the cathelicidin family containing a conserved cathelin domain and a variable C-terminus (Figure 2). Cathelicidin-NV shared the highest identity of 75% with the predicted Cath-2-like-isoform X1 from the frog *Nanorana parkeri*. Multisequence alignment of the cathelicidin-NV precursor with other amphibian cathelicidins (Supplementary Figure S2) indicated that the cathelicidin-NV precursor exhibits a high degree of similarity with the other cathelicidins in the cathelin regions, but they are highly variable in the C-terminal mature region. Additionally, a characteristic feature of all these mature peptides is the presence of one intramolecular disulfide bond.

Cathelicidin-NV lacks direct antimicrobial activity and shows no cytotoxicity and hemolytic activity toward mammalian cells

Among the 15 strains of the microorganisms tested (Supplementary Table S2), cathelicidin-NV did not show antimicrobial activity against Gram-positive bacteria (7 strains), Gram-negative bacteria (6 strains) and fungi (2 strains) at the concentration of 200 μg/ml (70.28 μM). Cathelicidin-NV did not exhibit cytotoxicity toward HSFs, HaCat cells and RAW264.7 at the concentration of 200 μg/ml. In addition, it did not have hemolytic activity against erythrocytes at the same concentration.

Cathelicidin-NV enhances proliferation and motility of keratinocytes and fibroblasts

The proliferation and motility of keratinocytes and fibroblasts are the most critical factors in wound healing, which promote the re-epithelialization process and accelerate wound closure. As illustrated in Figure 3A–C, cathelicidin-NV obviously enhanced the proliferation of HaCat and HSF cells in a concentration-dependent

```
atgaaggtctggcagtgtgcgctatggatctccgctctcacatggcaggcggctcgctct   60
M  K  V  W  Q  C  A  L  W  I  S  A  L  T  W  Q  A  A  R  S      20
cagtctccggatcgggaagaatggatcagagaggccttggatctctacaaccagagggaa  120
Q  S  P  D  R  E  E  W  I  R  E  A  L  D  L  Y  N  Q  R  E      40
gatggagagttcttctttaaattcctgtctgatctcccggccgcccccctggaggaggaa  180
D  G  E  F  F  F  K  F  L  S  D  L  P  A  A  P  L  E  E  E      60
aacaatccgacaatctcgttcttaataaaggagacggaatgcctgaaatctgaagatatc  240
N  N  P  T  I  S  F  L  I  K  E  T  E  C  L  K  S  E  D  I      80
aatttggaggaatgtgactacaagaaggacggggaggtgaaggtctgtggattgtacccg  300
N  L  E  E  C  D  Y  K  K  D  G  E  V  K  V  C  G  L  Y  P     100
gaggaggggagaccatgaagactttgaaatgtgtcagcctgaccaagaattttcacacc  360
E  E  G  E  T  M  K  T  L  K  C  V  S  L  T  K  N  F  H  T     120
aagcgtgccagaggtaagaaggaatgcaaggatgatcgctgtaggctgcttatgaaacgt  420
K  R  A  R  G  K  K  E  C  K  D  D  R  C  R  L  L  M  K  R     140
ggatcattcagctacgtttaaggcgtcgatttctgatcatcgcccggcgatcagctgtaa  480
G  S  F  S  Y  V  *                                            146
cgcacgcttgaagggacattccacccgaaactttttgtagctcttttgtcagatacgat  540
gctttatgttccgctacaattcagctgaatagttctgtacattgtatcccatgacgccaa  600
taaaatgaaagctttggcctcccaaaaaaaaaaaaaaaaaaaaaaaaaaaaaaa        652
```

Figure 2. The cDNA sequence of the cathelicidin-NV precursor.
Deduced amino acid sequence is shown below the cDNA sequence. The cathelicidin-NV precursor contains the signal peptide (*gray*), followed by a cathelin domain ending with a pair of basic residues (in *bold*), and the mature peptide (*black*). The stop codon is indicated by an *asterisk*. Amino acid numbers or nucleotide numbers are shown after the sequences.

manner. At the concentration of 20 µg/ml, the rates of proliferation were increased by 43% and 63% for HaCat and HSF cells, respectively. The scrambled version of cathelicidin-NV, called sNV, did not show any activities on the proliferation of keratinocytes and fibroblasts (Figure 3C,D and Supplementary Figure S3).

To observe the effect of cathelicidin-NV on keratinocyte migration, an *in vitro* cells scratch assay was performed. Cathelicidin-NV significantly promoted keratinocyte migration; as illustrated in Figure 3C,D, the migration of HaCaT cells across the wound chasm was significantly enhanced in cells treated with cathelicidin-NV compared with those treated with vehicle. The repair rate of scarification of cathelicidin-NV reached 51 or 74% at 24 or 48 h, respectively, but that of vehicle only reached 32 or 56% at 24 or 48 h, respectively (Figure 3C).

Cathelicidin-NV accelerates the healing of full-thickness wounds in mice

Considering that cathelicidin-NV has strong ability to promote proliferation and motility of keratinocytes and fibroblasts *in vitro*, we performed an excisional wound-healing mouse model to address whether topical application of cathelicidin-NV would modify the healing of full-thickness dermal wounds *in vivo*. The time course observations indicated that topical application of cathelicidin-NV and sCathelicidin-NV (synthetic cathelicidin-NV) (200 µg/ml, 20 µl) on mice significantly accelerated wound closure, compared with mice treated with vehicle and sNV control (Figure 4A,B). The sNV did not show any accelerated activities on the healing of full-thickness dermal wounds (Figure 4A,B). Cathelicidin-NV also showed effects on wound healing comparable to the positive control epidermal growth factor (EGF) (Figure 4A,B). Furthermore, there were obviously contractions of wounds in cathelicidin-NV-treated mice, compared with wounds treated with vehicle control or EGF (Figure 4A). On post-injury day 2, the wound area in cathelicidin-NV-treated mice was ~22% smaller than that in control mice (Figure 4B). Subsequently, there was a rapid acceleration of wound healing in cathelicidin-NV- and EGF-treated mice. On day 8, the wound treated with cathelicidin-NV or EGF was ~88 and 90% smaller than controls, respectively. On day 10, the wounds of cathelicidin-NV- and EGF-treated mice were almost closed completely, whereas the wounds of control mice remained ~6% (Figure 4A,B). No adverse effects on the body weight, general health or behavior of the mice were observed for the topical cathelicidin-NV treatment.
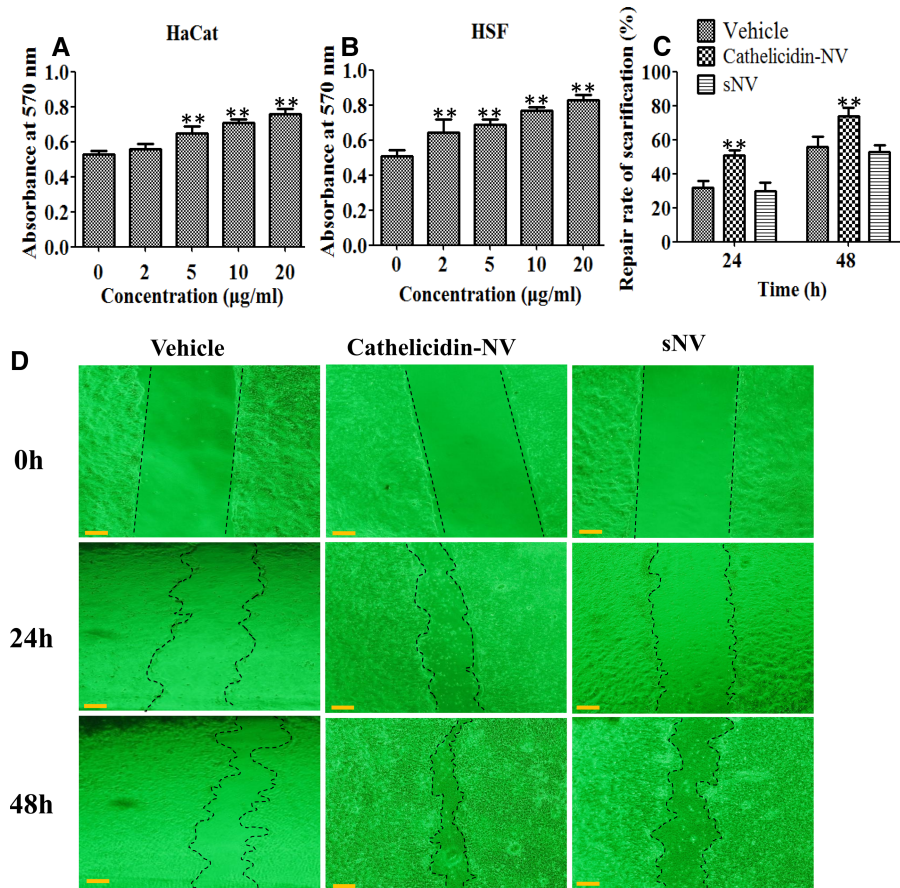
Figure 3. Cathelicidin-NV enhanced the proliferation and motility of keratinocytes and fibroblasts.
(**A** and **B**) Cultured keratinocytes (**A**) and fibroblasts (**B**) were treated with vehicle (Control) or cathelicidin-NV with indicated concentration and relative cell numbers were estimated by OD readings. (**C** and **D**) Effects of cathelicidin-NV and sNV on scratch wounding closure in cultured keratinocytes. (**C**) Quantification of the repair rate of scarification. (**D**) Representative images. Values are the mean ± SEM ($n = 5$). $**P < 0.01$ compared with control.

In a parallel experiment, we killed mice in cathelicidin-NV-treated and control groups at post-injury days 4 and 10, and then performed a histological evaluation of skin tissue sections stained with H&E. Cathelicidin-NV-treated mice exhibited enhanced restoration of dermal and epidermal and formation of granulation tissue in the wound (Figure 4C–E). The measurement of the distance between epithelial tongues revealed a clear enhancement of the re-epithelialization process in most of the cathelicidin-NV-treated wounds at days 4 and 10 post wounding (Figure 4C,D). The percentage of re-epithelialization was improved by 35% after 4 days, and by 26% after 10 days of treatment with cathelicidin-NV. At day 4, an increase in the lengths of the tongues of new migrating epithelium was clearly observed in cathelicidin-NV-treated wounds (Figure 4C,D). At day 10, a similar increase was observed, as in most cases the epithelial tongues had converged to completely cover the wound when cathelicidin-NV was applied, whereas in the corresponding vehicle wounds the epithelial gap was still evident (Figure 4C,D). Granulation tissue developed more slowly in control wounds, as the cell density in the central area of the 4,10-day cathelicidin-NV-treated wounds was higher than that of control wounds (Figure 4E).

Cathelicidin-NV induces fibroblast-to-myofibroblast transition and the production of collagen from fibroblasts in skin wound

Given the above observation that cathelicidin-NV obviously promoted the proliferation of HSFs *in vitro* and enhanced mice wound healing by contractions, we further explored the potential effect of cathelicidin-NV on fibroblasts in a skin wound. Fibroblast-to-myofibroblast transition plays an important role in cutaneous wound
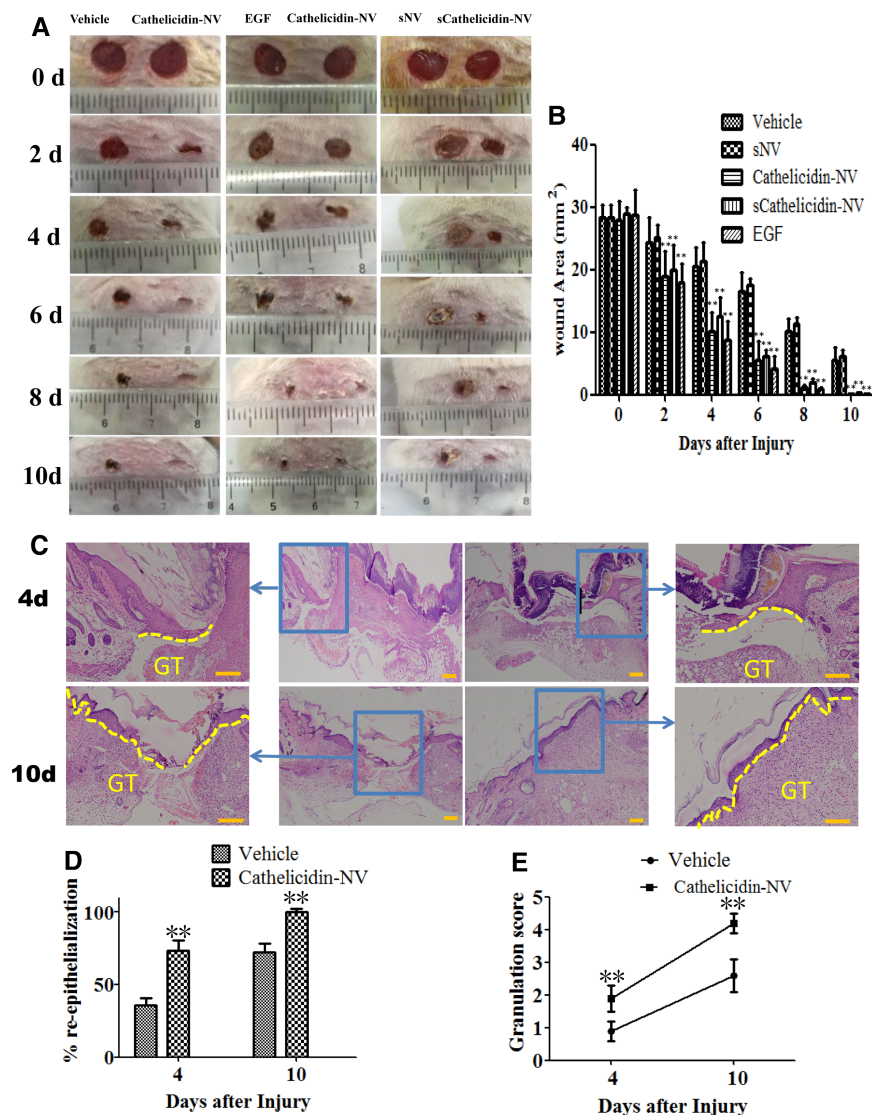
Figure 4. Topical application of cathelicidin-NV accelerated the healing of full-thickness wounds in mice.

(**A**) Images of a representative mouse from each group taken on post-injury days 0, 2, 4, 6, 8 and 10 are shown. Two full-thickness skin wounds of 6-mm diameter were created on the back of each mouse wound, and closure was monitored by the painted application of vehicle, cathelicidin-NV (20 μl, 20 μg/ml), EGF (20 μl, 100 μg/ml), sNV or sCathelicidin-NV (synthetic cathelicidin-NV). (**B**) Wound area at different days post injury. Values represent mean ± SEM ($n = 10$ per group). **$P < 0.01$ compared with control. (**C**) Images of skin tissue sections stained with H&E at days 4 and 10 post wounding. (The yellow dotted line: the neo-epithelium, GT: indicates granulation tissue, Scale bar = 100 μm). (**D**) Percent re-epithelialization at days 4 and 10 post wounding. (**E**) Histological scores of granulation thickness at days 4 and 10 post wounding. Values represent mean ± SEM ($n = 6$ per group). **$P < 0.01$ compared with control.

healing [25]. In wound tissues at post-injury day 4, 10 myofibroblasts were stained brown with an antibody against alpha-smooth muscle actin (α-SMA), a differentiation marker of smooth muscle cells. As illustrated in Figure 5A,B, there is strong expression of α-SMA in myofibroblasts of the granulation tissue below the wound surface at days 4 and 10 in cathelicidin-NV-treated mice, but only very weak signals in vehicle-treated mice. There was ~43 and 20% α-SMA positive area in the wound tissue of mice treated with cathelicidin-NV and vehicle, respectively, on day 4; then the proportion of the α-SMA positive area reached ~76 and 47%, respectively, on day 10 (Figure 5B). The result indicates that cathelicidin-NV obviously induces the fibroblast-to-myofibroblast transition.
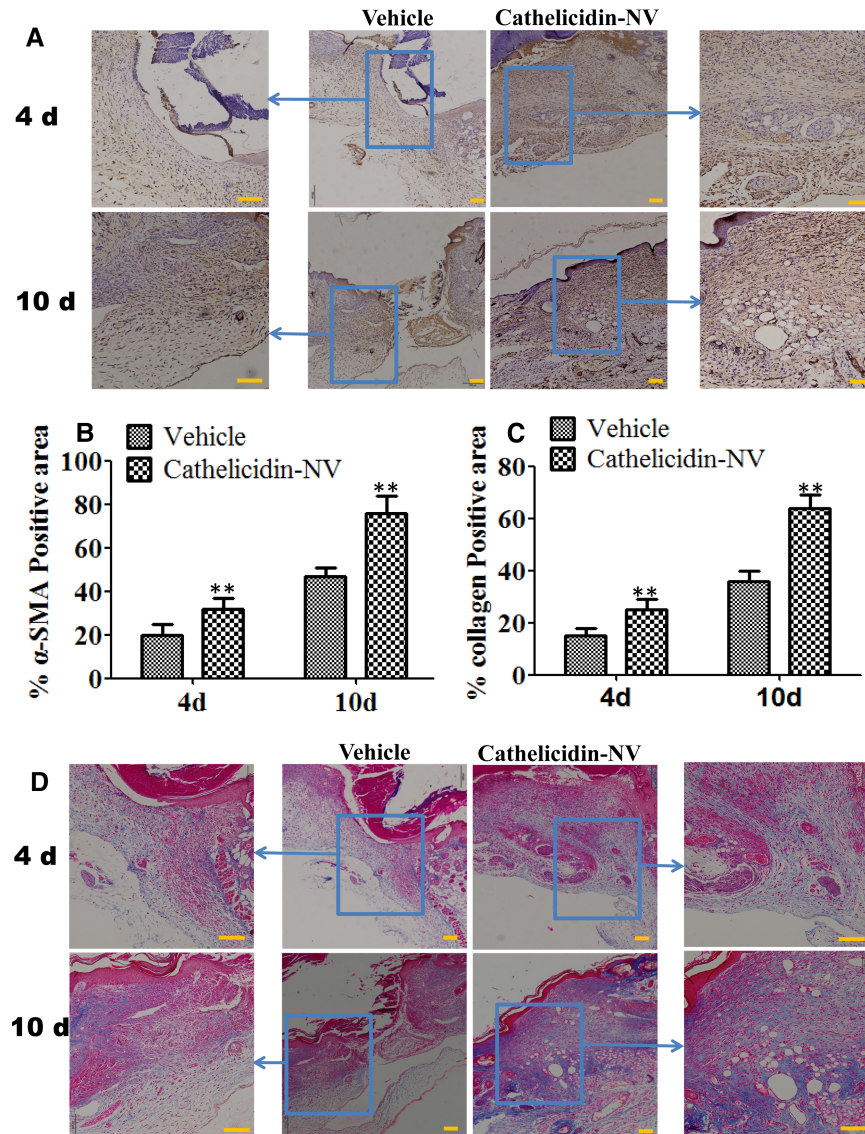
Figure 5. Cathelicidin-NV induced fibroblast-to-myofibroblast transition and significantly increased the production of collagen in the skin wound.

(**A**) The expression of α-SMA in wound skin treated with cathelicidin-NV or vehicle at days 4 and 10 after wounding. Myofibroblast are stained brown. (**B**) Quantification of α-SMA positive area. (**C**) Quantification of collagen positive area. (**D**) Histological assessment of collagen in the healing wounds. At days 4 and 10 post wounding, wounds with Vehicle and Cathelicidin-NV were stained for collagen with Masson Trichrome. Collagen bundles are stained blue. Scale bar = 200 μm. The IPLab imaging software were used to measure the changes of the wound. All values represent mean ± SEM (*n* = 6 per group). *******P* < 0.01 compared with control.

To further examine collagen deposition from fibroblasts in the wounds, wound tissues at post-injury days 4 and 10 were stained with Masson trichrome. The wounds in the cathelicidin-NV-treated mice contain higher levels of collagen, both on day 4 and day 10, compared with the vehicle-treated wounds, respectively (Figure 5C,D); the percentage of collagen positive area was improved by 65% after 4 days, and by 77% after 10 days of treatment with cathelicidin-NV (Figure 5C).

Effects on cytokine secretion *in vitro* and *in vivo*

Wound healing is a complex biological process that is regulated by numerous growth factors, cytokines and chemokines. To determine the effect of cathelicidin-NV on cytokine and chemokine secretion *in vitro*, we used
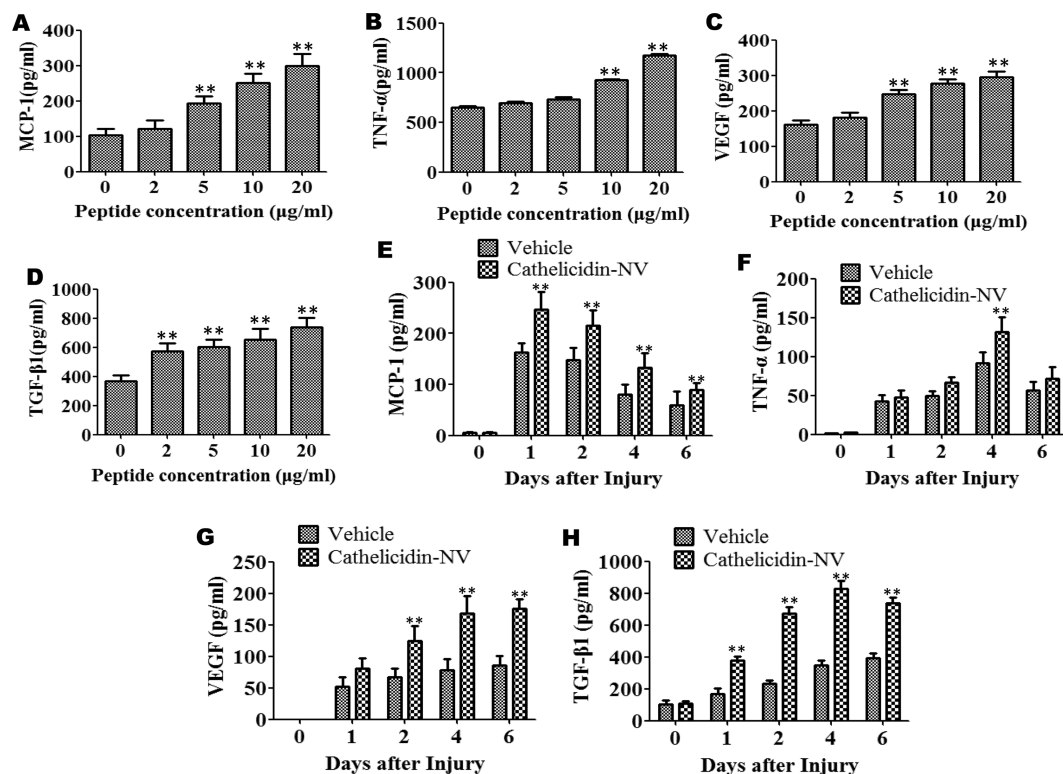
Figure 6. Cathelicidin-NV induced MCP-1, TNF-α, VEGF and TGF-β1 secretion in murine macrophages cell line RAW264.7 and skin wound.

(A–D): Cathelicidin-NV significantly increased MCP-1, TNF-α, VEGF and TGF-β1 secretion in a dose-dependent manner in the culture supernatants of RAW264.7. (**E–H**) Cathelicidin-NV significantly increased the expression of MCP-1, TNF-α, VEGF and TGF-β1 in the wound site at the indicated day after injury. Values represent mean ± SEM ($n = 6$ per group). **$P < 0.01$ compared with control.

ELISA to measure the MCP-1, TNF-α, VEGF and TGF-β1 level in murine macrophage cell line RAW264.7. As illustrated in Figure 6A–D, cathelicidin-NV significantly increased MCP-1, TNF-α, VEGF and TGF-β1 secretion in a dose-dependent manner in the culture supernatants of RAW264.7.

Furthermore, to determine cathelicidin-NV on cytokine and chemokine secretion at the wound site, wounds were harvested 0, 1, 2, 4 and 6 days after wounding, homogenized and analyzed using ELISA kits. All of the tested proteins in the pointed day were expressed at higher levels in cathelicidin-NV-treated wounds than in vehicle-treated wounds (Figure 6E–H). Overall, these results show that cathelicidin-NV significantly induced expression of several cytokines and chemokines *in vitro* and *in vivo,* which are related with wound healing.

Effects of cathelicidin-NV on MAPKs

Western immunoblot analysis was performed to further explore the effect of cathelicidin-NV on the MAPK signaling pathway in RAW 264.7 macrophage cells. As illustrated in Figure 7A–D cathelicidin-NV significantly increased ERK and p38 phosphorylation in a concentration-dependent manner, but showed little effect on JNK phosphorylation. After a 1 h treatment with 2, 5, 10 and 20 μg/ml tylotoin, ERK phosphorylation was increased by 0.1, 0.6, 1.3 and 1.8 times, while the corresponding p38 up-regulation was 1.0, 2.4, 3.2 and 3.4 times, respectively.

Discussion

The classical model of wound healing is a highly complex, orchestrated and overlapping process that can be divided into four main phases: hemostasis, inflammation, proliferation and tissue remodeling [26–28]. Chronic wounds, defined as a barrier defect that has not healed in an orderly set of phases or in a timely fashion, have become a major therapeutic challenge [29]. Thus, identifying more effective wound therapies (medicines) of treating chronic wounds is urgently necessary. Amphibian skins display excellent wound-healing ability and
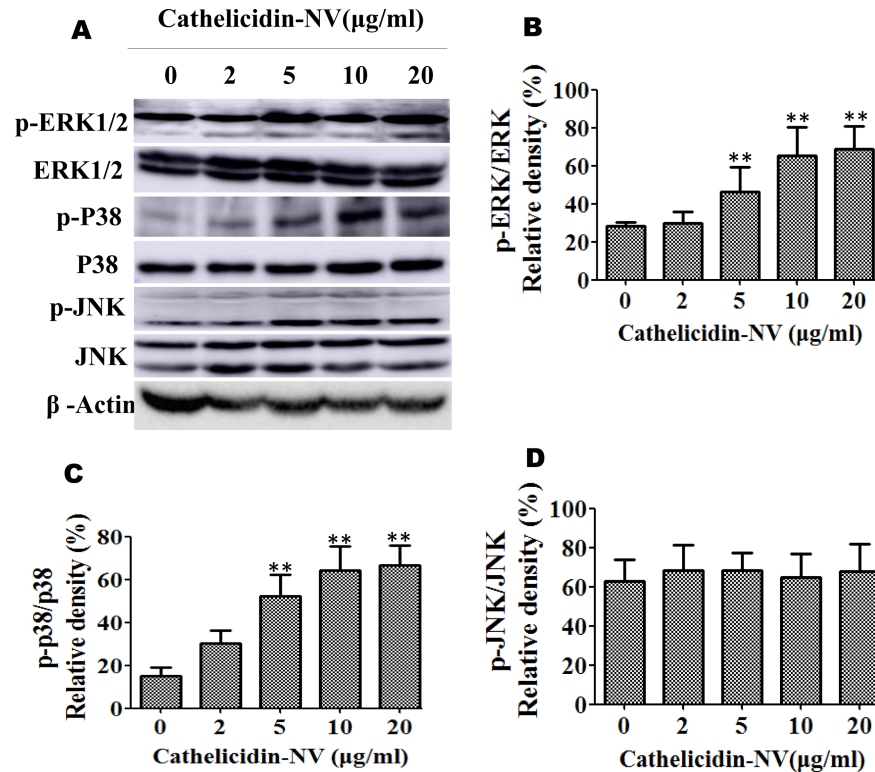
Figure 7. Effects of tylotoin on MAPK signaling pathways.

(**A–D**) Western blot showed effects of cathelicidin-NV on ERK, JNK and p38 protein kinase phosphorylation (**A**) and relative activation analysis (**B–D**). The results were quantified by ImageJ. The densitometry of phosphorylated ERK, JNK and p38 were normalized to total ERK, JNK and p38, and graphed as the mean ± SEM ($n = 5$). The values with treatment by cathelicidin-NV are significantly different from the values for the control (**$P < 0.01$).

represent a resource for prospective wound healing-promoting peptides. As a step toward understanding amphibians' wound healing and identifying novel wound healing peptides, we address this issue and have characterized a potential wound healing-promoting peptide (cathelicidin-NV) from *N. ventripunctata* in this work.

Cathelicidin-NV is a short peptide (ARGKKECKDDRCRLLMKRGSFSYV) and is composed of just 24 amino acid residues. The precursor of cathelicidin-NV belongs to the cathelicidin family, which are a unique and diverse group of effector molecules involved in humoral immunity among vertebrates. Cathelicidin-NV is a highly basic peptide with a net charge of +5, which is an important parameter contributing to the ability of cationic peptides to bind to and disrupt microbial membranes. However, cathelicidin-NV did not have any direct effect on fifteen strains of microorganisms at concentrations up to 200 µg/ml, including 7 strains of Gram-positive bacteria, 6 strains of Gram-negative bacteria and 2 strains of fungi (Supplementary Table S2). In addition, it showed no cytotoxicity and hemolytic activity toward mammalian cells at the same concentration of 200 µg/ml (Data not shown). The synthetic cathelicidin-NV (sCathelicidin-NV) with one intramolecular disulfide bond exhibited the same bioactivity *in vitro* and *in vivo* with the purified cathelicidin-NV from the skin secretions (Figure 4A,B and Supplementary Figure S3), which further confirmed the structure of cathelicidin-NV. Moreover, the scrambled version of cathelicidin-NV (sNV) did not show any activities on the motility and proliferation of keratinocytes and fibroblasts (Figure 3C,D and Supplementary Figure S3). Cathelicidin-NV seems to be a specific wound healing-promoting peptide.

Wound healing after damage to the skin involves a complex interplay of primarily keratinocytes, fibroblasts, endothelial cells of vessels, recruited immune cells and their associated extracellular matrix [29]. The proliferation, migration and differentiation of these cells resulted in the formation of new tissue and ultimately wound closure [26,30]. Re-epithelialization is a crucial process, which entails re-covering the surface of the wound with new epithelium and requires proper migration and proliferation of keratinocytes at the periphery of the wound [31].

Cathelicidin-NV treatment markedly enhanced the proliferation and motility of keratinocytes (Figure 3A–D) *in vitro*. Further *in vivo* investigations demonstrated that cathelicidin-NV can effectively promote cutaneous wound healing (Figure 4A–E). Topical application of cathelicidin-NV greatly accelerated full-thickness skin wound healing in a mouse model of a full-thickness skin wound (Figure 4A,B). Accelerated wound closure was observed in the mice treated with cathelicidin-NV compared with vehicle control. As illustrated in Figure 4C,D, cathelicidin-NV directly accelerated re-epithelialization of the wound site. In addition to re-epithelialization resulting from the proliferation and motility of keratinocytes, fibroblasts are also important repairing cells that dominantly take part in the proliferation phase of wound healing. Some of fibroblasts differentiate into myofibroblasts and these contractile cells will help bridge the gap between the wound edges [32]. As illustrated in Figure 5A,B, cathelicidin-NV significantly promoted the expression of α-SMA *in vivo*, a differentiation marker of smooth muscle cells, suggesting that cathelicidin-NV accelerated the fibroblast-to-myofibroblast transition to accelerate wound closure. Additionally, cathelicidin-NV was found to significantly induce collagen production from fibroblasts in the skin wound as illustrated in Figure 5C,D, which is essential for the formation of granulation tissue. Taken together, cathelicidin-NV obviously promotes the formation of granulation tissue by inducing proliferation of fibroblasts (Figure 3B), fibroblast-to-myofibroblast transition (Figure 5A,B) and collagen production from fibroblasts (Figure 5C,D). Meanwhile, cathelicidin-NV directly enhances the proliferation of keratinocyte cells, resulting in accelerated re-epithelialization of the wound site. The results suggest that a more efficient wound-healing process in mice treated with cathelicidin-NV might result from enhanced proliferation, differentiation and secretion of fibroblasts in the injured area, which facilitate the formation of granulation tissue.

Macrophages almost take part in every process during wound healing and they provide a continual source of growth factors. They can produce many cytokines associated with wound healing such as VEGF, MCP-1, TNF-α and TGF-β1 [32], which are important producers of inflammatory mediators. VEGF and MCP-1 are known to promote angiogenesis in wounds, and this vascularization in the wound-bed area is important for the proper supply of nutrients and oxygen to allow rapid growth of the skin [33–35]. TNF-α is also able to influence the rate of wound healing through regulation of a smooth muscle actin expression in dermal fibroblasts [36]. TGF-β1 is a multifunctional cytokine that plays important roles in cell proliferation, differentiation and especially in formation of extracellular matrix (ECM) [37]. Our results indicated that cathelicidin-NV has an effect on cytokine and chemokine secretion *in vitro* and *in vivo*. As illustrated in Figure 6A,D, cathelicidin-NV significantly increased MCP-1, TNF-α, VEGF and TGF-β1 secretion in a dose-dependent manner in the culture supernatants of RAW264.7 *in vitro*. Furthermore, cathelicidin-NV also significantly up-regulated MCP-1, TNF-α, VEGF and TGF-β1 levels in wounds *in vivo* (Figure 6E–H). MCP plays an important role in wound-healing processes, which chemotactically attracts neutrophils and monocytes into the wound [11]. The monocytes differentiate into macrophages, which initiate the development of granulation tissue and release a variety of pro-inflammatory cytokines and growth factors contributing to wound healing [38]. Additionally, cathelicidin-NV was found to induce VEGF secretion as illustrated in Figure 6C,G. VEGF can enhance endothelial cell migration and proliferation to stimulate angiogenesis, which plays a critical role in wound healing [39], because it provides nutrients, oxygen and wound-healing factors to enter the wound area.

Our results are partially different from the other two amphibian cathelicidins (tylotoin and cathelicidin-OA1) that showed similar wound-healing effects. Tylotoin increased TGF-β1 and IL-6 secretion in a dose-dependent manner in the culture supernatants of RAW264.7 and it had no significant effect on IL-1β, EGF and TNF-α secretion [17]. Cathelicidin-OA1 promoted the secretion of TNF-α and TGF-β in the human monocyte-like cell line THP-1 [18], and the authors did not detect the effect of cathelicidin-OA1 on other cytokines and chemokines. Additionally, the human cathelicidin LL-37, which was the best characterized member of the cathelicidin family, has been shown to exhibit wound healing-promoting activities *in vitro* and *in vivo*. LL-37 increased the production of cytokines and chemokines such as IL-6, IL-8, TNF-α, IL-10, MCP-1, interferon-inducible protein-10 (IP-10) and macrophage inflammatory protein-3 alpha (MIP3a) in keratinocytes [40,41]. Moreover, the wound-healing activity of LL-37 could be mediated not only through the transactivation of the epidermal growth factor receptor (EGFR) but also through the induction of formyl peptide receptor-like 1 (FPRL-1) expression in human keratinocyte cell line HaCaT [23]. Cathelicidin-NV belongs to the cathelicidin family and its functions seem to overlap with those of the mammalian counterparts. The structure and activity relationship for cathelicidin-NV needs to be further investigated.

The MAPK signaling system has been demonstrated to take an important role in wound healing [42–44]. Western blot analysis showed that cathelicidin-NV significantly increased the activation of the ERK and p38 subgroups of the MAPK signaling pathway in a concentration-dependent manner (Figure 7A–C). This

demonstrated that both the ERK and p38 signaling pathways are involved in cathelicidin-NV-stimulated cytokines related with wound healing release, and they may have a cross-talk and orchestrate in regulating these cytokines' expression and wound-healing process.

In conclusion, cathelicidin-NV identified from *N. ventripunctata* skin is a bioactive/effector compound with potential wound-healing ability. It promotes the proliferation of fibroblasts, the differentiation of fibroblasts to myofibroblasts and collagen production in fibroblasts. Furthermore, it also promotes the secretion of cytokines and chemokines *in vivo* and *in vitro*, including MCP-1, TNF-α, VEGF and TGF-β1. It may facilitate the understanding of frog wound healing and skin regeneration. In addition, these properties make cathelicidin-NV a potent candidate for skin wound therapeutics.

Abbreviations

DMEM, Dulbecco's modified Eagle's medium; EGF, epidermal growth factor; ELISA, enzyme-linked immunosorbent assay; ERK, extracellular regulated protein kinases; FBS, fetal bovine serum; H&E, Hematoxylin and Eosin; HSFs, human skin fibroblasts; JNK, c-Jun NH2-terminal kinase; MALDI-TOF, matrix-assisted laser desorption ionization time-of-flight; MAPK, mitogen-activated protein kinases; MCP-1, monocyte chemoattractant protein-1; MTT, 3-(4,5-dimethylthiazol-2-yl)-2,5-diphenyl-2H-tetrazolium bromide; p38, p38 mitogen-activated protein kinases; PBS, phosphate-buffered saline; RP-HPLC, reversed-phase high-performance liquid chromatography; TGF-β1, transforming growth factor-β1; TNF-α, tumor necrosis factor-α; VEGF, vascular endothelial growth factor; α-SMA, α-smooth muscle actin.

Author Contribution

J.W., L.M. and H.Y. conceived and designed the experiments and analyzed the data. J.W., L.M., H.Y., J.Y., L.W., X.W., K.M., Y.S., and T.L. performed the experiments. L.M. and H.Y. contributed reagents/materials/analysis tools and wrote the paper. All the authors read and approved the final version of the manuscript.

Competing Interests

The Authors declare that there are no competing interests associated with the manuscript.

References

1   Yang, H., Wang, X., Liu, X., Wu, J., Liu, C., Gong, W. et al. (2009) Antioxidant peptidomics reveals novel skin antioxidant system. *Mol. Cell. Proteomics* **8**, 571–583 https://doi.org/10.1074/mcp.M800297-MCP200

2   Campbell, L.J. and Crews, C.M. (2008) Wound epidermis formation and function in urodele amphibian limb regeneration. *Cell. Mol. Life Sci.* **65**, 73–79 https://doi.org/10.1007/s00018-007-7433-z

3   Yokoyama, H., Maruoka, T., Aruga, A., Amano, T., Ohgo, S., Shiroishi, T. et al. (2011) Prx-1 expression in *Xenopus laevis* scarless skin-wound healing and its resemblance to epimorphic regeneration. *J. Invest. Dermatol.* **131**, 2477–2485 https://doi.org/10.1038/jid.2011.223

4   Ferris, D.R., Satoh, A., Mandefro, B., Cummings, G.M., Gardiner, D.M and Rugg, E.L. (2010) Ex vivo generation of a functional and regenerative wound epithelium from axolotl (Ambystoma mexicanum) skin. *Dev. Growth Differ.* **52**, 715–724 https://doi.org/10.1111/j.1440-169X.2010.01208.x

5   Gennaro, R., Skerlavaj, B. and Romeo, D. (1989) Purification, composition, and activity of two bactenecins, antibacterial peptides of bovine neutrophils. *Infect Immun.* **57**, 3142–3146 PMID:2777377

6   Zaiou, M. and Gallo, R.L. (2002) Cathelicidins essential gene-encoded mammalian antibiotics. *J. Mol. Med.* **80**, 549–561 https://doi.org/10.1007/s00109-002-0350-6

7   Xiao, Y., Cai, Y., Bommineni, Y.R., Fernando, S.C., Prakash, O., Gilliland, S.E. et al. (2006) Identification and functional characterization of three chicken cathelicidins with potent antimicrobial activity. *J. Biol. Chem.* **281**, 2858–2867 https://doi.org/10.1074/jbc.M507180200

8   Zhao, H., Gan, T.-X., Liu, X.-D., Jin, Y., Lee, W.-H., Shen, J.-H. et al. (2008) Identification and characterization of novel reptile cathelicidins from elapid snakes. *Peptides* **29**, 1685–1691 https://doi.org/10.1016/j.peptides.2008.06.008

9   Mu, L., Zhou, L., Yang, J., Zhuang, L., Tang, J., Liu, T. et al. (2017) The first identified cathelicidin from tree frogs possesses anti-inflammatory and partial LPS neutralization activities. *Amino Acids* **49**, 1571–1585 https://doi.org/10.1007/s00726-017-2449-7

10   Zhang, X.-J., Zhang, X.-Y., Zhang, N., Guo, X., Peng, K.-S., Wu, H. et al. (2015) Distinctive structural hallmarks and biological activities of the multiple cathelicidin antimicrobial peptides in a primitive teleost fish. *J. Immunol.* **194**, 4974–4987 https://doi.org/10.4049/jimmunol.1500182

11   Burton, M.F. and Steel, P.G. (2009) The chemistry and biology of LL-37. *Nat. Prod. Rep.* **26**, 1572–1584 https://doi.org/10.1039/b912533g

12   Gonzalez-Curiel, C., Trujillo, V., Montoya-Rosales, A., Rincon, K., Rivas-Calderon, B., DeHaro-Acosta, J. et al. (2014) 1,25-dihydroxyvitamin d3 induces LL-37 and HBD-2 production in keratinocytes from diabetic foot ulcers promoting wound healing: an *in vitro* model. *PLoS ONE* **9**, e111355 https://doi.org/10.1371/journal.pone.0111355

13 Salvado, M.D., Di Gennaro, A., Lindbom, L., Agerberth, B. and Haeggstrom, J.Z. (2013) Cathelicidin LL-37 induces angiogenesis via PGE2-EP3 signaling in endothelial cells, *in vivo* inhibition by aspirin. *Arterioscler. Thromb. Vasc. Biol.* **33**, 1965–1972 https://doi.org/10.1161/ATVBAHA.113.301851

14 Aarbiou, J., Tjabringa, G.S., Verhoosel, R.M., Ninaber, D.K., White, S.R., Peltenburg, L.T. et al. (2006) Mechanisms of cell death induced by the neutrophil antimicrobial peptides α-defensins and LL-37. *Inflamm. Res.* **55**, 119–127 https://doi.org/10.1007/s00011-005-0062-9

15 Dombrowski, Y. and Schauber, J. (2012) Cathelicidin LL-37: a defense molecule with a potential role in psoriasis pathogenesis. *Exp. Dermatol.* **21**, 327–330 https://doi.org/10.1111/j.1600-0625.2012.01459.x

16 Hao, X., Yang, H., Wei, L., Yang, S., Zhu, W., Ma, D. et al. (2012) Amphibian cathelicidin fills the evolutionary gap of cathelicidin in vertebrate. *Amino Acids* **43**, 677–685 https://doi.org/10.1007/s00726-011-1116-7

17 Mu, L., Tang, J., Liu, H., Shen, C., Rong, M., Zhang, Z. et al. (2014) A potential wound-healing-promoting peptide from salamander skin. *FASEB J.* **28**, 3919–3929 https://doi.org/10.1096/fj.13-248476

18 Cao, X., Wang, Y., Wu, C., Li, X., Fu, Z., Yang, M. et al. (2018) Cathelicidin-OA1, a novel antioxidant peptide identified from an amphibian, accelerates skin wound healing. *Sci. Rep.* **8**, e1005943 https://doi.org/10.1038/s41598-018-19486-9

19 Liu, H., Duan, Z., Tang, J., Lv, Q., Rong, M. and Lai, R. (2014) A short peptide from frog skin accelerates diabetic wound healing. *FEBS J.* **281**, 4633–4643 https://doi.org/10.1111/febs.12968

20 Liu, H., Mu, L., Tang, J., Shen, C., Gao, C., Rong, M. et al. (2014) A potential wound healing-promoting peptide from frog skin. *Int. J. Biochem. Cell Biol.* **49**, 32–41 https://doi.org/10.1016/j.biocel.2014.01.010

21 Tang, J., Liu, H., Gao, C., Mu, L., Yang, S., Rong, M. et al. (2014) A small peptide with potential ability to promote wound healing. *PLoS ONE* **9**, e92082 https://doi.org/10.1371/journal.pone.0092082

22 Wei, L., Che, H., Han, Y., Lv, J., Mu, L., Lv, L. et al. (2015) The first anionic defensin from amphibians. *Amino Acids* **47**, 1301–1308 https://doi.org/10.1007/s00726-015-1963-8

23 Carretero, M., Escámez, M.J., García, M., Duarte, B., Holguín, A., Retamosa, L. et al. (2008) *In vitro* and *in vivo* wound healing-promoting activities of human cathelicidin LL-37. *J. Invest. Dermatol.* **128**, 223–236 https://doi.org/10.1038/sj.jid.5701043

24 Rebalka, I.A., Raleigh, M.J., D'Souza, D.M., Coleman, S.K., Rebalka, A.N. and Hawke, T.J. (2015) Inhibition of PAI-1 via PAI-039 improves dermal wound closure in diabetes. *Diabetes* **64**, 2593–2602 https://doi.org/10.2337/db14-1174

25 Gabbiani, G. (2003) The myofibroblast in wound healing and fibrocontractive diseases. *J. Pathol.* **200**, 500–503 https://doi.org/10.1002/path.1427

26 Singer, A.J. and Clark, R.A. (1999) Cutaneous wound healing. *N. Engl. J. Med.* **341**, 738–746 https://doi.org/10.1056/NEJM199909023411006

27 Cotran, R.S., Kumar, V. and Collins, T. (1999) Wound healing. In *Robbins Pathologic Basis of Disease* (Kumar, V., ed.), pp. 107–111, W.B. Saunders Company, Philadelphia, USA.

28 Li, J., Chen, J. and Kirsner, R. (2007) Pathophysiology of acute wound healing. *Clin. Dermatol.* **25**, 9–18 https://doi.org/10.1016/j.clindermatol.2006.09.007

29 Martin, P. and Nunan, R. (2015) Cellular and molecular mechanisms of repair in acute and chronic wound healing. *Br. J. Dermatol.* **173**, 370–378 https://doi.org/10.1111/bjd.13954

30 Barrientos, S., Stojadinovic, O. and Golinko, M.S. (2008) Growth factors and cytokines in wound healing. *Wound Repair Regen.* **16**, 585–601 https://doi.org/10.1111/j.1524-475X.2008.00410.x

31 Santoro, M.M. and Gaudino, G. (2005) Cellular and molecular facets of keratinocyte reepithelization during wound healing. *Exp. Cell Res.* **304**, 274–286 https://doi.org/10.1016/j.yexcr.2004.10.033

32 Rodero, M.P. and Khosrotehrani, K. (2010) Skin wound healing modulation by macrophages. *Int. J. Clin. Exp. Pathol.* **3**, 643–653 PMID:20830235

33 Leibovich, S.J., Polverini, P.J., Fong, T.W., Harlow, L.A. and Koch, A.E. (1994) Production of angiogenic activity by human monocytes requires an L-arginine/nitric oxide-synthase-dependent effector mechanism. *Proc. Natl Acad. Sci. U.S.A.* **91**, 4190–4194 https://doi.org/10.1073/pnas.91.10.4190

34 Frank, S., Hübner, G., Breier, G., Longaker, M.T., Greenhalgh, D.G. and Werner, S. (1995) Regulation of vascular endothelial growth factor expression in cultured keratinocytes. Implications for normal and impaired wound healing. *J. Biol. Chem.* **270**, 12607–12613 https://doi.org/10.1074/jbc.270.21.12607

35 Salcedo, R., Ponce, M.L., Young, H.A., Wasserman, K., Ward, J.M. and Kleinman, H.K. (2000) Human endothelial cells express CCR2 and respond to MCP-1: direct role of MCP-1 in angiogenesis and tumor progression. *Blood* **96**, 34–40 PMID:10891427

36 Goldberg, M.T., Han, Y.-P., Yan, C., Shaw, M.C. and Garner, W.L. (2007) TNF-α suppresses α-smooth muscle actin expression in human dermal fibroblasts: an implication for abnormal wound healing. *J. Invest. Dermatol.* **127**, 2645–2655 https://doi.org/10.1038/sj.jid.5700890

37 Kopecki, Z., Luchetti, M.M., Adams, D.H., Strudwick, X., Mantamadiotis, T., Stoppacciaro, A. et al. (2007) Collagen loss and impaired wound healing is associated with c-Myb deficiency. *J. Pathol.* **211**, 351–361 https://doi.org/10.1002/path.2113

38 Jiang, Y.-Y., Xiao, W., Zhu, M.-X., Yang, Z.-H., Pan, X.-J., Zhang, Y. et al. (2012) The effect of human antibacterial peptide LL-37 in the pathogenesis of chronic obstructive pulmonary disease. *Respir. Med.* **106**, 1680–1689 https://doi.org/10.1016/j.rmed.2012.08.018

39 Park, J., Hwang, S. and Yoon, I.-S. (2017) Advanced growth factor delivery systems in wound management and skin regeneration. *Molecules* **22**, 1259 https://doi.org/10.3390/molecules22081259

40 Braff, M.H., Hawkins, M.A., Di Nardo, A., Lopez-Garcia, B., Howell, M.D., Wong, C. et al. (2005) Structure-function relationships among human cathelicidin peptides: dissociation of antimicrobial properties from host immunostimulatory activities. *J. Immunol.* **174**, 4271–4278 https://doi.org/10.4049/jimmunol.174.7.4271

41 Niyonsaba, F., Ushio, H., Nakano, N., Ng, W., Sayama, K., Hashimoto, K. et al. (2007) Antimicrobial peptides human β-defensins stimulate epidermal keratinocyte migration, proliferation and production of proinflammatory cytokines and chemokines. *J. Invest. Dermatol.* **127**, 594–604 https://doi.org/10.1038/sj.jid.5700599

42 Lee, J.C., Laydon, J.T., McDonnell, P.C., Gallagher, T.F., Kumar, S., Green, D. et al. (1994) A protein kinase involved in the regulation of inflammatory cytokine biosynthesis. *Nature* **372**, 739–746 https://doi.org/10.1038/372739a0

43 Muthusamy, V. and Piva, T.J. (2010) The UV response of the skin: a review of the MAPK, NFκB and TNFα signal transduction pathways. *Arch. Dermatol. Res.* **302**, 5–17 https://doi.org/10.1007/s00403-009-0994-y

44 Schett, G., Zwerina, J. and Firestein, G. (2008) The p38 mitogen-activated protein kinase (MAPK) pathway in rheumatoid arthritis. *Ann. Rheum. Dis.* **67**, 909–916 https://doi.org/10.1136/ard.2007.074278